Journal of Radiological Protection

Official journal of the Society for Radiological Protection

PAPER

Benchmarking point-kernel method against Monte Carlo simulations for an ALARA case study in occupational radiation protection

To cite this article: Federica Roberto *et al* 2025 *J. Radiol. Prot.* **45** 041508

View the article online for updates and enhancements.

You may also like

- Special section: Selected papers from the Fourth International Workshop on Recent Advances in Monte Carlo Techniques for Radiation Therapy
Jan Seuntjens, Luc Beaulieu, Issam El Naqa et al.
- Monte Carlo Calculations in Nuclear Medicine: Applications in Diagnostic Imaging
C A Giannone
- Full Atomistic Kinetic Monte Carlo and First Principles Study on Electromotive Force of SOFC with Direct Counting Approach
Tomofumi Tada

This content was downloaded from IP address 193.190.185.205 on 04/11/2025 at 12:56

IOP Publishing J. Radiol. Prot. 45 (2025) 041508 https://doi.org/10.1088/1361-6498/ae16b5

Journal of Radiological Protection

Check for updates

PAPER

RECEIVED
27 August 2025

REVISED
8 October 2025

ACCEPTED FOR PUBLICATION
23 October 2025

PUBLISHED
4 November 2025

Benchmarking point-kernel method against Monte Carlo simulations for an ALARA case study in occupational radiation protection

Federica Roberto[1,2,*], **Mahmoud Abdelrahman**[1], **Lombardo Pasquale**[1], **Filip Vanhavere**[1] and **John A Lee**[2]

[1] SCK CEN, Belgian Nuclear Research Center, Boeretang 190, Mol, 2400, Belgium
[2] Université Catholique de Louvain, Louvain-la-Neuve, Belgium
[*] Author to whom any correspondence should be addressed.

E-mail: federica.roberto@sckcen.be

Keywords: radiation protection, ALARA, point-kernel, Monte Carlo, benchmarking

Abstract

The principle of as low as reasonably achievable (ALARA) is of paramount importance for the radiation protection of workers, and more specifically in the context of the decommissioning of nuclear facilities. For that purpose, several tools have been developed to measure and assess radiation doses to workers, to plan radiological work, and to ensure that safety protocols are followed. Most of these planning tools are based on the well-established point-kernel (PK) method, while others rely on Monte Carlo (MC) simulations. The scope of this paper is to compare, for some case studies, the performance and accuracy of VISIPLAN 4.0, a PK-based tool developed at SCK CEN, with MC simulations, to highlight the advantages and limitations of both methods. The major advantage of PK methods is usually related to their lower computational burden, at the cost of a less accurate assessment of dose values. However, depending on the number of source points chosen for the PK method, the simulation time could be comparable to MC simulations: in the scenarios presented in this paper, the simulation time was comparable to MC simulations when a high number of source points was considered. Moreover, VISIPLAN, on average, overestimated the dose assessment by approximately 50% compared to MC results.

1. Introduction

The decommissioning of nuclear facilities is an activity that will increase in the upcoming years worldwide. The dismantling of nuclear facilities differs in its nature from routine tasks performed under normal operating conditions. Therefore, workers will face other types of radiation exposure and hazards, compared to normal operations, that require specific handling of activity planning [1]. The principle of as low as reasonably achievable (ALARA), and the planning tools that rely on it, plays an important role within the framework of decommissioning and dismantling at different stages, including preparation and design phases, implementation, follow-up, and feedback analysis. In order to address the first stage, predictive tools are needed to estimate individual and collective exposures, to compare and select optimal options for achieving the dosimetric goals [2]. Both dose rate measurements and computational methods are used to assess worker exposures, while the latter are mostly based on two main approaches: point-kernel (PK) methods and Monte Carlo (MC) simulations.

PK methods are deterministic methodologies used for radiation transport and dose assessment, via a two-step calculation process. In the first stage they calculate the un-collided flux of gamma rays using, for example, ray tracing techniques: the dose at a point is determined by accounting for the distance travelled by the radiation through the materials encountered in the trajectory and the attenuation properties of the materials. In the second stage, the primary dose is multiplied by buildup factors (BUFs) to consider the impact of scattered and secondary photons [3]: these correction factors are tabulated values,

© 2025 Society for Radiological Protection. Published on behalf of SRP by IOP Publishing Limited. All rights, including for text and data mining, AI training, and similar technologies, are reserved.

which vary with the energy of photons, the shield material, and the penetration depth. PK methods are based on a linear superposition of point source responses, assuming straight-line attenuation and applying empirical buildup corrections. However, they are not suitable for complex scatter geometries, particle regeneration (e.g. Bremsstrahlung), anisotropic fields, and other complex interactions. Well-established tools based on the PK method are, for example, VISIPLAN [4], MicroShield [5], and VRDOSE [6].

On the other hand, MC simulations are stochastic methods based on the random generation of samples from a certain probability distribution relevant to the physical problem under evaluation. In the case of particle transport, for example in the radiation protection framework, MC codes are used to simulate the interactions of a large number of particles with matter, based on cross-sectional data, over a wide range of energies and in complex three-dimensional (3D) geometries [7]. Particles are tracked through random interactions, with probabilistic models, including scattering, absorption, secondary particles' generation, and other particles' physical laws. Some of the most used MC codes are MCNP [8], Geant4 [9], and PHITS [10].

Due to the intrinsic nature of the two methodologies, the provided results differ in accuracy and computational effort. MC codes provide highly accurate results for complex geometries and interactions, which require significant computational resources. In contrast, deterministic methods provide direct solutions to transport equations, often with less computational effort, but may be less accurate for highly complex or anisotropic problems. The characteristics of the two methodologies have already been compared and reported by [11, 12], mentioning a difference of 20%–30% between the results of the two methodologies. Both articles focus in particular on the role of BUFs considering a single detection point in simple geometrical configurations, stating the inadequacy of PK methods when considering more than one BUF simultaneously in complex geometrical conditions. Therefore, within the framework of dose assessment for decommissioning and ALARA planning, the limitation of PK calculations can affect dose estimation in various situations, particularly in highly complex or anisotropic environments. As a result, it can lead to an inadequate dose assessment and consequent planning of the work.

The objective of the present work is to compare the two methodologies to highlight their advantages and limitations and to help in the decision-making process of the most suitable calculation method for each situation considered. Unlike previous studies, this work aims to calculate and compare the accumulated dose and computational effort for a more complicated scenario. A worker is following predefined paths in a realistic facility where several sources and shielding materials are present. Moreover, the worker body is simulated using the ICRP phantom [13]: its advantage is the accuracy of dose estimation in a scenario including different irradiation directions. The ICRP reference computational phantoms are used for calculating organ absorbed doses from ionising radiations. The male and female phantoms are 3D digital models based on computed tomography (CT) scans of real individuals, and they are suited for reproducing human organs and tissues as a 3D array of cuboid voxels, such that each entry in the array identifies the organ or tissue to which the corresponding voxel belongs. The MC and PK codes selected for the comparison are PHITS 3.31 [10] and VISIPLAN 4.0 [4], respectively. PHITS 3.31 has been selected because of its broad range of types of particle and energies coverage, its simpler structure of input and output files, and since it is free for research and educational use with respect to other available MC tools. The version chosen was the latest available when the simulations were run. Regarding VISIPLAN 4.0, it has been considered as a representative ALARA tool based on PK methodology, selected due to its availability to SCK CEN employees.

2. Methodology description

The element that is at the base of the analysis of this case study is a standard 220 l barrel for the temporary storage of radioactive waste. The barrel is filled with concrete, contains radioactive isotopes, and is enclosed by a carbon steel casing. The density and element composition of the different materials involved are defined following the definition of VISIPLAN 4.0 and are accordingly adapted in PHITS. Two representative isotopes were considered as radioactive gamma sources: ^{137}Cs and ^{60}Co, having isotropic emission and homogeneous distribution inside the barrel. Comparable configurations were introduced in the two tools: the two isotopes were divided into the two halves of the barrels, with ^{137}Cs and ^{60}Co placed in the bottom and top half of the barrel, respectively. Different levels of activity were included. Following the investigation approach in [11, 12], simple case studies were first introduced, to establish the performance of the two methodologies at an increasing level of complexity of the scenario.

First, an example was introduced considering a single barrel to analyse the consequence of the choice of the BUF considered for the dose assessment. As mentioned previously, the choice of the BUF is of primary importance in the configuration of VISIPLAN parameters, since only one BUF can be chosen in each simulation, although more materials are present in the geometry. In this preliminary study, the

phantom was placed at increasing distances from a single barrel containing a homogeneously distributed high-activity source (activity equal to 3.62×10^8 Bq for ^{137}Cs and 2.94×10^9 Bq for ^{60}Co). This example, hereafter referred to as Case A for simplicity, was made to check the dose trend with different BUFs at increasing distances, while maintaining fixed sources and shielding.

Moreover, an additional complexity step was introduced (Case B). With the same configuration of a barrel containing a homogeneously distributed source (activity equal to 3.62×10^8 Bq for ^{137}Cs and 2.94×10^9 Bq for ^{60}Co) and the phantom located at 1 m distance, a concrete wall of 30 cm thickness was placed between these two elements.

The results of the two methodologies for these initial case studies are discussed in the following section.

Another parameter that must be correctly selected in the VISIPLAN configuration is the number of sampling points for the volumetric source distribution inside the barrel. In MC, it is possible to configure the source as homogeneously distributed, which means that the source particles are generated inside the whole volume in which the source is defined. Normally, the number of source particles generated is in the order of millions or billions, ensuring the complete fill of the whole volume and a reliable statistic of the results. On the other hand, the maximum number of points that VISIPLAN can randomly sample inside a volumetric source is equal to 32 000. However, it is not common practice to set this parameter at its maximum value, for time-saving purposes: developers recommend the use of 1 point source per litre of volume of the drum, which is, in this case, equal to 220 source points for the 220 l drum. In this context, three different numbers of points have been chosen for comparison: 1 point source placed in the middle of each half of the barrel (simplest configuration), 110 point sources placed in each half of the barrel (recommended configuration), and 32 000 point sources placed in each half of the barrel (closest to MC configuration). Again, the results of the different source configurations in VISIPLAN are discussed in the results, referred to as Case C.

Finally, the more complex scenario was simulated. The latter is reproducing a real temporary storage facility: it consists of a large room (20 m long, 8 m wide, 5 m high) that includes a total number of 50 barrels, grouped in different locations, containing radioisotopes at different levels of activity. In the room a sliding lead wall is also present, which divides the room in two areas where barrels with lower activity and barrels with higher activity are separated. The sliding door has the function of opening and closing once the worker is entering and exiting, respectively, the separated space at the bottom of the main room. In this case, the different levels of activity were arbitrarily set as high (3.62×10^8 Bq for ^{137}Cs and 2.94×10^9 Bq for ^{60}Co), medium (2.01×10^8 Bq for ^{137}Cs and 1.56×10^8 Bq for ^{60}Co) and low (3.0×10^6 Bq for ^{137}Cs and 1.0×10^7 Bq for ^{60}Co), within each half barrel. The configuration of the room and the placement of the barrels with their specific activities are schematically reported in figure 1. The worker's task is to move the barrel with the highest activity (H), in the lower left corner of figure 1, to another location for future transportation, choosing between two different paths. The locations along the first path are drawn in figure 2, while figure 3 shows the locations along the second path. The sliding lead wall is represented open in every sub-figure, while in the simulations each time the worker crosses the sliding door, the latter opens or closes accordingly. The worker enters and exits through the same gate, on the right, and different colours were assigned to the trajectories to highlight whether the worker is carrying a barrel or not, and the activity level of the carried barrel, if any. The green trajectories represent the segments of the path where the worker is not carrying any barrels, whereas to the other trajectories it has been assigned the same colour as the one of the barrel carried by the worker in that segment, since each colour refers to an activity level of the carried barrel. In each sub-figure, the barrels are reported in the final location where they are carried at the end of the trajectories represented in that specific sub-figure. These two paths were evaluated as alternative ways to move the high activity drum from its corner location, being surrounded by other barrels of different levels of activity: in Path 1 the medium activity barrel is first removed, while in Path 2 the low activity ones are removed before reaching the target barrel. The two alternatives were expected to give different results, which is important from the ALARA point of view. To mimic the carriage of the barrel, the phantom (PHITS) or the detection point (VISIPLAN) was set 50 cm away from the external surface of the barrel. In VISIPLAN, the detection points were located at a height of 120 cm, to mimic the location where the physical dosimeter is normally worn by the worker in operation. The numbers reported in the sub-figures refer to the positions of the phantom (for PHITS configuration case) and of the detection point (for VISIPLAN configuration case) along the path, in sequential order. It was assumed that the time spent at each location on the trajectories was equal to 60 s where the worker was not carrying any barrel, and equal to 120 s where a barrel was carried.

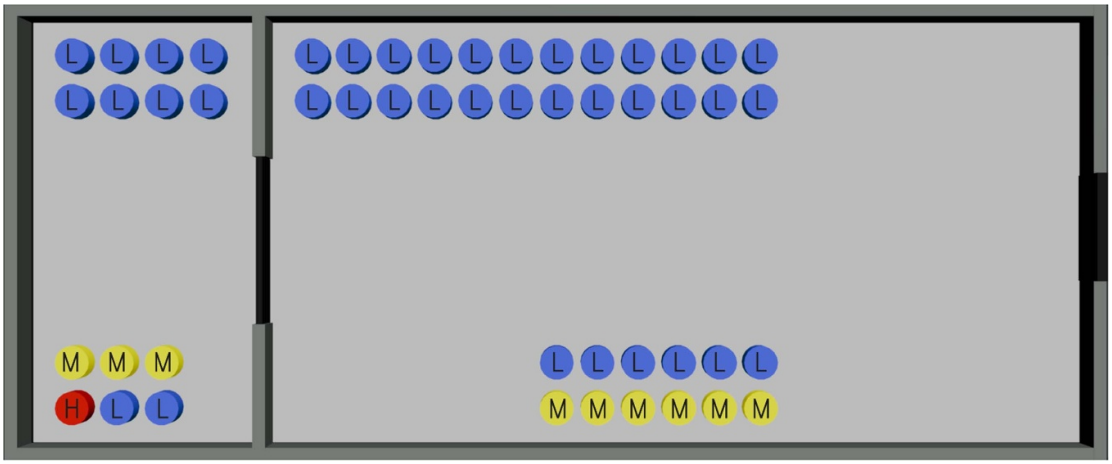
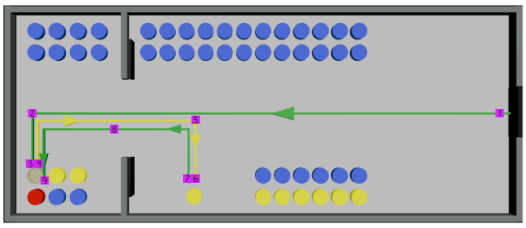
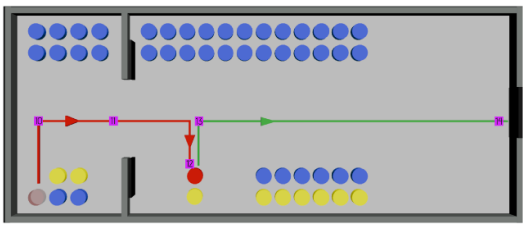


Figure 1. Configuration of the room where the worker is performing the activity under evaluation. Distribution of barrels based on the sources activity: low (L), medium (M), and high (H).

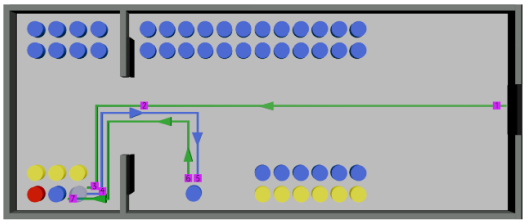


(a) First part of Path 1: move the medium activity drum (in front of the high activity one) to the group of 12 barrels on the other side of the room.

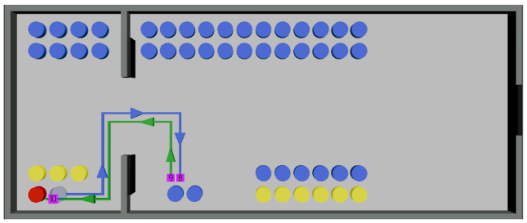


(b) Second part of Path 1: move the target drum to the final location and leave the room.

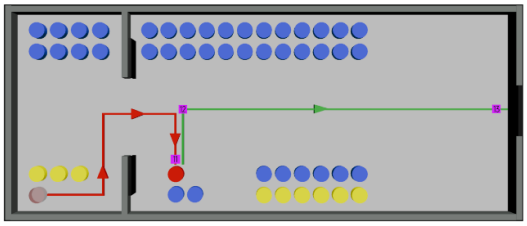
Figure 2. Path 1 divided into 14 visited locations.



(a) First part of Path 2: move one low activity barrel from the side of high activity one to the group of 12 barrels on the other side of the room.



(b) Second part of Path 2: move another low activity barrel on the side of high activity one to the group of 12 barrels on the other side of the room.



(c) Third part of Path 2: move the target drum to the final location and leave the room.

Figure 3. Path 2 divided into 13 visited locations.

Notably, although the scenarios presented are more complicated than those in the literature, they cannot be considered as detailed as a real case of a facility under decommissioning. In real-case scenarios, sources are commonly not homogeneously distributed in the drums, with disparities such as hot spots or several, often unknown, materials inside each drum and heterogeneously distributed.

Table 1. Tissue weighting factors, w_T.

Tissue	w_T	$\sum w_T$
Red bone marrow, colon, lung, stomach, breast, remainder tissues[a]	0.12	0.72
Gonads	0.08	0.08
Bladder, oesophagus, liver, thyroid	0.04	0.16
Endosteum (bone surface), brain, salivary glands, skin	0.01	0.04
Total		1.00

Source: [14, 16].

[a] Remainder tissues: adrenals, extrathoracic region, gall bladder, heart, kidneys, lymphatic nodes, muscle, oral mucosa, pancreas, prostate (male), small intestine, spleen, thymus, and uterus/cervix (female).

The definition of radiation protection quantities and units has been described by [14], among others, where a system of dose measures is reported to relate different types of quantities for the practical assessment of doses. Although MC is a flexible code that can provide any quantity for radiation protection, directly or indirectly, VISIPLAN is restricted to the calculation of the effective dose, which belongs to the so-called *protection quantities* group. Therefore, the effective dose E is the quantity that has been compared between the two methods, even if calculated differently for the two codes and explained in more detail in the corresponding section.

The final objective of the described scenarios is to compare the exposure in each path between the two methods and retrieve the differences. Moreover, the simulation time is compared between the two tools for all the case studies proposed.

2.1. PHITS configuration

The general configuration of geometry and source definition described in the previous paragraph was integrated in the corresponding sections of the PHITS input files. For each position at increasing distance in the preliminary case studies and for each visited location by the worker along the two paths, the ICRP phantom [13] was placed at that specific location to obtain the effective dose value E. The phantom also rotates based on which side of the room it is facing in each location: for this reason, each location and rotation angle of the worker in the room was run in a different simulation.

Moreover, for time-saving purposes, PHITS simulations were run as long as the *r.err* of the equivalent dose rate in the air region surrounding the phantom reached 2%. This region was selected to avoid too small regions of the phantom and preserve a certain accuracy on the results retrieved by PHITS over the phantom regions.

For the preliminary case study, not only the ICRP phantom was introduced to obtain the effective dose E, but the *operational quantity* ambient dose equivalent $H^*(10)$ was calculated for comparison. $H^*(10)$ is an *operational quantity* for measurements in external radiation fields, related to the physical radiation field quantity *fluence* through the corresponding dose conversion coefficient [15].

2.1.1. ICRP phantom

In this paper, the male reference phantom of ICRP was considered, which consists of all major organs and tissues of an average adult male body (141 regions in total). Based on the latter, the reference formula to calculate the effective dose E (Sv) is [14]:

$$E = \sum_{T} w_T H_T = \sum_{T} w_T \sum_{R} w_R D_{T,R} \quad , \tag{1}$$

which requires a few calculation steps. The value of the absorbed dose for each phantom region $D_{T,R}$ (Gy) represents the outcome of PHITS simulations, therefore multiplied by the radiation weighting factor ($w_R = 1$ for photons) to retrieve the equivalent dose in an organ or tissue H_T (Sv). Since only photons were considered, the sum over radiation types (R) was not necessary. The equivalent dose must then be multiplied by the tissue weighting factor (w_T, different for each tissue), leading to the final value of the effective dose E (Sv). The groups of tissues considered by the ICRP and the relative weighting factor are reported in table 1 [14].

It can be observed that the number of groups mentioned in table 1 does not match the 141 tissues and organs proposed as ICRP phantom by PHITS. These regions must be correctly classified into

the different groups of tissues, following the PHITS developers' instructions. More detailed information can be found in the ICRP Publication 110 [13]. Once the correct weighting factor w_T was associated with each phantom region, the mass (g) of the region has been calculated, given its density and volume. Therefore, the mass of each region was multiplied by the equivalent dose H_T (Sv) and divided by the masses of all other regions that belong to the same subgroup of tissues (e.g. if adrenals are considered, their mass is divided by the masses of all the tissues catalogued as remainder tissues). The results were then summarised by tissue subgroups, and for each subgroup the corresponding tissue weighting factor w_T was multiplied. Finally, the values of $w_T H_T$ were summed to calculate the effective dose E (Sv). Throughout this process, the propagation of the error was also taken into account, starting from the *r.err* associated with the absorbed dose retrieved by PHITS simulations, which was inserted into:

$$\sigma_E = \sqrt{\sum_{i=1}^{t} w_{T,i}^2 w_R^2 \mathrm{coeff}(A,B)_j^2 \, \sigma_{D_{(T,R)_j}}^2}, \tag{2}$$

where

- $w_{T,i}$ is the tissue weighting factor of the group of tissues i,
- w_R is the radiation weighting factor, equal to 1 since only photons were considered,
- $\mathrm{coeff}(A,B)_j$ is the mass (g) of the organ/tissue j divided by the total mass of the tissues T included in the correspondent group of tissue weighting factor $w_{T,i}$,
- $\sigma_{D_{(T,R)_j}}$ is the standard deviation associated to the absorbed dose rate on the organ/tissue j, $D_{(T,R)_j}$ $(\mathrm{Gy\,h^{-1}})$, such that

$$\sigma_{D_{(T,R)_j}}^2 = \left(r.\mathrm{err} \cdot \sigma_{D_{(T,R)_j}}\right)^2 . \tag{3}$$

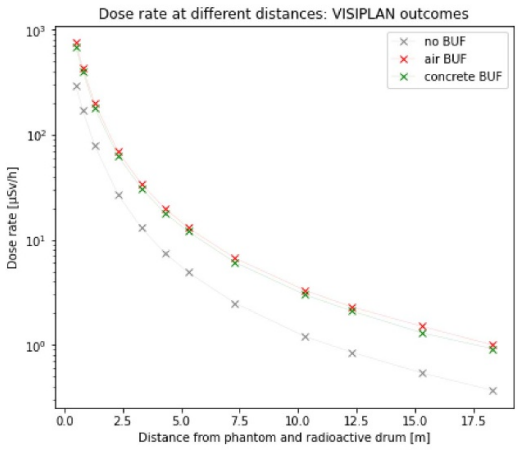
2.2. VISIPLAN configuration

The calculations in the VISIPLAN 4.0 ALARA tool are based on a 3D model of the workplace that includes geometry, materials, and source information, which are introduced in a user-friendly interface. Calculations are based on the PK technique using an infinite-media buildup correction according to Taylor's formula fitting [17]. In order to compare the two tools, the same configurations entered in the PHITS simulations were set in VISIPLAN: the same geometry, materials, source isotopes and activities, and source distributions were integrated. Concerning the source, the possible number of sampling points for the source distribution setting has already been discussed in the methodology section (Case C), and the results of this study, with its consequent choice, will be later reported. Moreover, for dose assessment, VISIPLAN 4.0 can include or not the BUF of different materials in the calculation, and only one BUF at a time can be considered in each simulation. Therefore, if the user wants to calculate the dose for different BUFs (for the same configuration), the code must be run once for each BUF of interest. The parameters included for the calculation of the BUFs in VISIPLAN refer to the document ANSI/ANS-6.4.3-1991 [18]. For this case study, it was decided to run each simulation independently considering every BUF, for all the materials present in a certain scenario, for comparison of the results. However, a couple of observations for the choice of the correct BUF should be added:

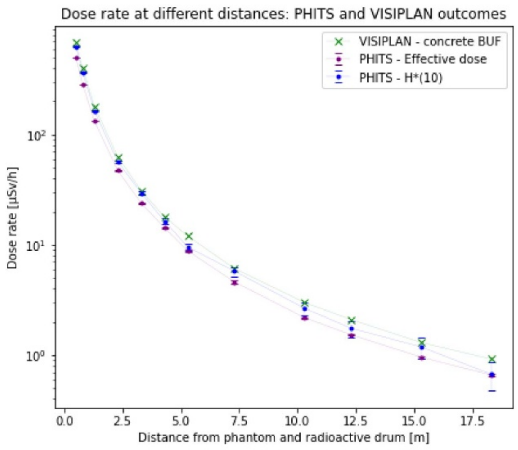
- The chosen BUF is applied to the entire distance between the source point and the detection point, and not exclusively to the segment that is crossing the material corresponding to the chosen BUF. If, for example, the source point is located in the middle of a barrel of *radius* = 0.3 m, filled with concrete, and the detection point is located at 4.7 m from the surface of the barrel, in a room containing air, the chosen BUF will be applied to the 5 m distance between the source point and the detection point for any chosen BUF.
- The way to choose the correct BUF is recommended by the developers: it should be chosen among the most relevant mean free path *mfp* of the materials encountered between the source point and the detection point. The *mfp* (–) is defined as the attenuation coefficient of a material ($\mu(E)$ $(\mathrm{cm^{-1}})$) multiplied by the distance travelled by the particles in that material. The values of μ are discretized by the energy (E) of the particles that cross the material, therefore, they should be chosen accordingly. Considering the example just mentioned, the *mfp* for each material will be:

  – Concrete: 1.5×10^{-1} $(E = 1\,\mathrm{MeV})\,(\mathrm{cm^{-1}}) * 30\,(\mathrm{cm}) = 4.5$
  – Air: 7.75×10^{-5} $(E = 1\,\mathrm{MeV})\,(\mathrm{cm^{-1}}) * 470\,(\mathrm{cm}) = 3.6 \times 10^{-2}$

  Therefore, the concrete BUF was chosen since the corresponding *mfp* is higher.



(a) Effective dose rate with different applied BUF: VISIPLAN results.



(b) Dose rate: PHITS and VISIPLAN results.

Figure 4. Case A. Phantom at increasing distance from stand-alone drum: PHITS and VISIPLAN results.

Calculating the effective dose in VISIPLAN requires the use of dose conversion coefficients, to relate the protection quantity *effective dose* to the physical radiation field quantity *fluence* [13]. These dose conversion coefficients were taken from the Corrigenda to ICRP Publication 116 [19] and manually added into the software. Eventually, different irradiation geometries can be considered for the effective dose calculation in VISIPLAN 4.0, although each configuration requires a separate simulation run. In this example, it was decided to consider mainly the rotational (ROT) irradiation geometry. The latter is extensively described in [14], as the geometry that assumes an isotropic rotational exposure of the body about the vertical axis. It is used to represent situations where the person either rotates in the field or is exposed to a radiation field that is symmetric around the vertical axis of the body. Therefore, the ROT irradiation geometry appeared to be suitable for many of the phantom locations in the proposed scenarios, which include several sources located around the trajectory of the phantom. In contrast, in the locations where the phantom is carrying the barrel, or it is directly facing the only barrel present in the room (Cases A, B, C), the anterior–posterior (AP) irradiation geometry (ionising radiation is incident on the front of the body in a direction orthogonal to its long axis) was taken into account. Vice versa, posterior–anterior irradiation geometry (ionising radiation is incident on the back of the body in a direction orthogonal to its long axis) was considered when the phantom turns its back to the drum [14]. In VISIPLAN, the effective dose was calculated at a detection point, which corresponded to the location where the phantom was placed in PHITS simulations, and was located at a height of 120 cm.

It must be noted that the approaches considered by the two methodologies were not perfectly coinciding, since the VISIPLAN dose assessment included the dose conversion coefficients approach, while the PHITS dose assessment considered the weighted sum of the energy deposited by the particles on each organ of the phantom. However, the choice of these irradiation geometries was made to be ideally closer to the effective dose calculated by post-processing of PHITS outcomes, based on the ICRP phantom implementation.

3. Results and discussion

The results of Case A, the study regarding the phantom placed at an increasing distance from the stand-alone barrel for the comparison of different BUFs in the VISIPLAN formulation, are first analysed. In figure 4 the outcomes of both methodologies for this case study are reported.

In figure 4(a), the effective dose rate values E (μSv h^{-1}) (AP irradiation geometry) calculated by VISIPLAN 4.0 are illustrated for the different applied BUFs: either without the application of BUF and with air and concrete BUFs. Although the results for air BUF and concrete BUF were almost aligned, with a difference of 10% in value between the two, excluding the application of the BUF led to an underestimation of up to 60% with respect to the application of concrete BUF. Obviously, avoiding the selection of any BUF value leads to an incorrect formulation of the problem, and among the selection of concrete or air BUF, the choice was driven by the recommendation given by the VISIPLAN developers. Therefore, in the following discussion it has been decided that only the concrete BUF is considered, to

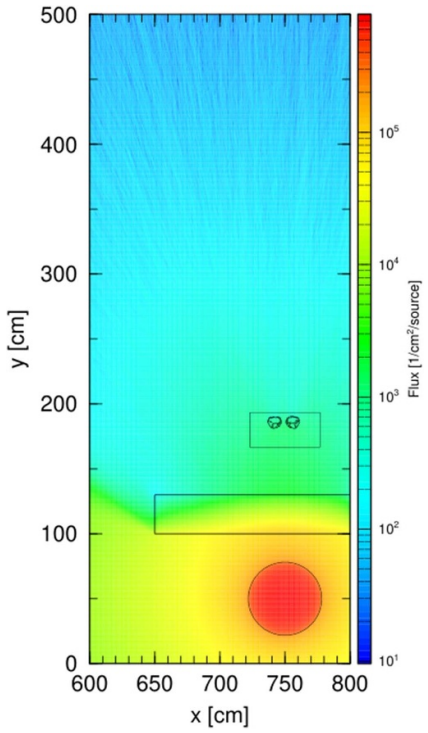


Figure 5. Case B. PHITS simulation: fluence distribution and geometry of the case study with a source barrel, a concrete shielding wall and a phantom located at 1 m distance.

improve readability. In figure 4(b) the effective dose rate E (μSv h^{-1}) and the ambient dose rate equivalent $H^*(10)$ (μSv h^{-1}) for PHITS version 3.31 (with the corresponding error bar) and VISIPLAN 4.0 for concrete BUF are reported. The difference between the protection quantity E and the operational quantity $H^*(10)$, reported in this graph, was approximately 20%, while the difference between the effective dose E calculated by the two methodologies was around 35% on average. The results of both methodologies follow the well-known radiation attenuation law, which states that the intensity decreases with the inverse square of the distance.

The additional test called Case B was presented above, placing a concrete wall of 30 cm thickness between the barrel and the phantom. This geometrical configuration is illustrated in figure 5, where the fluence distribution is also visible as an outcome of the PHITS simulation.

The presence of the shield increased the difference between the results of the two methodologies by 15%, compared to the results without the concrete shield between the source and the measurement point located at 1 m distance from the surface of the barrel. Eventually, it led to an overall overestimation of 50% between the VISIPLAN (concrete BUF) and the PHITS results.

The last parameter on which a specific analysis was required in VISIPLAN was the number of random sampling points for the volumetric distribution of the source within the barrel, presented as Case C. The results for the three numbers of sampling points considered (1, 110, 32 000) in VISIPLAN are reported in figure 6.

Between the extreme cases considering 1 point and maximum number of points (32 000 for VISIPLAN and homogeneously distributed for PHITS), both codes showed a 70% – 80% higher dose when the source was homogeneously distributed in the volume of the barrel with respect to the single point source (detection point at 1 m distance) within the results of the same methodology. This is explained by the fact that with 1 point source located in the middle of a barrel filled with concrete, the radiation attenuation increases with the presence of a larger portion of concrete. On the other side, if the source is distributed homogeneously in volume, and therefore has some source points closer to the surface of the barrel, a lower portion of concrete is present between the source points and the detection point. Regarding VISIPLAN, in the 1 point source case, the simulation time was negligible, while PHITS simulations required 8% less time with respect to the volumetric source configuration, on average. If for the case with 32 000 points the discrepancy between the effective dose E in PHITS and VISIPLAN (with concrete BUF) was 36% at 1 m distance, for the case with 1 point source the discrepancy reached 55%.

Between the 32 000 and 110 points source distribution configurations, VISIPLAN results showed a dose underestimation of 7% in the case of the 110 sampling points relative to the 32 000 sampling points

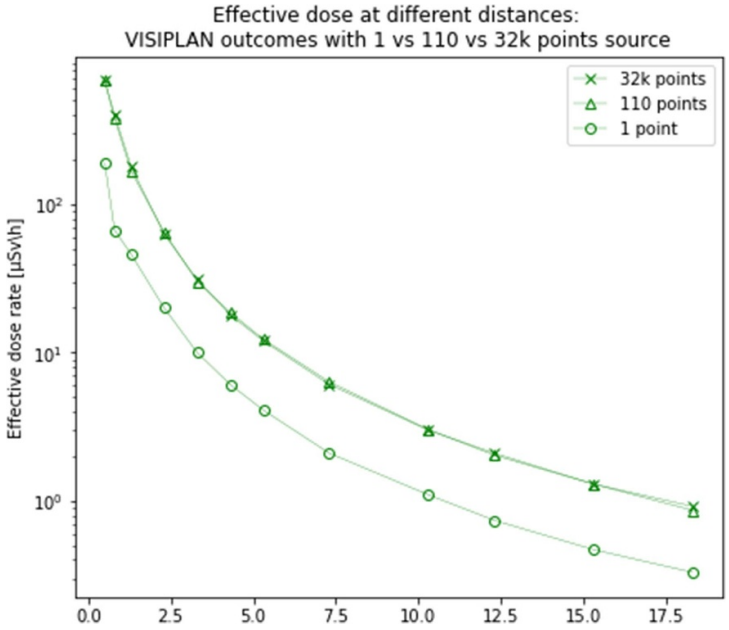


Figure 6. Case C. Dose rate at different distance for different numbers of source sampling points: VISIPLAN results.

source (at the distance of 1 m). Overall, the configuration with 110 sampling source points was almost aligned with the one having the maximum number of available sampling points. Moreover, the simulation time in VISIPLAN was almost negligible also in this case. Nevertheless, an additional observation on the 110 sampling points source distribution should be made: these points were randomly distributed inside the volume, therefore, at short distance locations, this led to different results at each run. For this reason, the same configuration was run six times, arbitrarily, and the results reported in figure 6 are the average values of these runs. Specifically, the variability of the results reached values of 43% at a certain distance.

Eventually, the source was consequently implemented considering the 32 000 random sampled points, in order to be coherent with the PHITS configuration of a volumetric source distribution and to avoid the variability of the results given by the 110 recommended value, when considering a short distance between the source and detection locations.

After these preliminary analyses, the results of the more complicated scenarios are discussed, regarding the two trajectories of the worker in the facility with multiple sources.

The effective dose E (μSv) for PHITS version 3.31 (with the corresponding error bar) and the results of VISIPLAN 4.0 considering only the concrete BUF are reported in figures 7 and 8 for the first and second investigated path, respectively. The comprehensive results of the two representative methodologies chosen are reported in table 2. In table 2 the total time spent by the worker on the two different paths is also indicated. For both methodologies, the path leading to the least exposure for the worker was Path 2: both methods agreed on the optimal path.

In general, VISIPLAN results were quite conservative compared to PHITS results, and the relative difference between the two methods can be observed in detail in figures 9 and 10: in both cases, VISIPLAN results overestimated PHITS results of 50% on average. As expected, VISIPLAN 4.0 tends to be a conservative methodology for assessing the dose of workers in decommissioning operations, which can lead to dose overestimation and inefficient time allocation of workers on site. However, this statement can be considered true for the case study here analysed, and it should be noticed that both methodologies arrived at the same choice of preferring Path 2, therefore coinciding in an ALARA context.

The general overestimation of the results of VISIPLAN 4.0 compared to the PHITS outcomes could be partly explained by the fact that VISIPLAN can include only one BUF of a certain material in the assessment of the dose. The issue of not being able to integrate the BUFs of all of the involved materials at the same time could lead to an accumulation of approximations in the calculation, at increasing distance and number of involved materials. The discrepancies observed in the result of the standalone example presented above, regarding the presence of a concrete wall between the source and the phantom, Case B, are illustrative in this sense. The presence of the wall increased the disagreement between the result of 15% relative to the same case without the shielding wall, at the same distance. Discrepancies could become larger, especially in the cases where the sliding walls shielded the locations of the phantom with respect to the source at high activity, as presented in the complex scenario inside

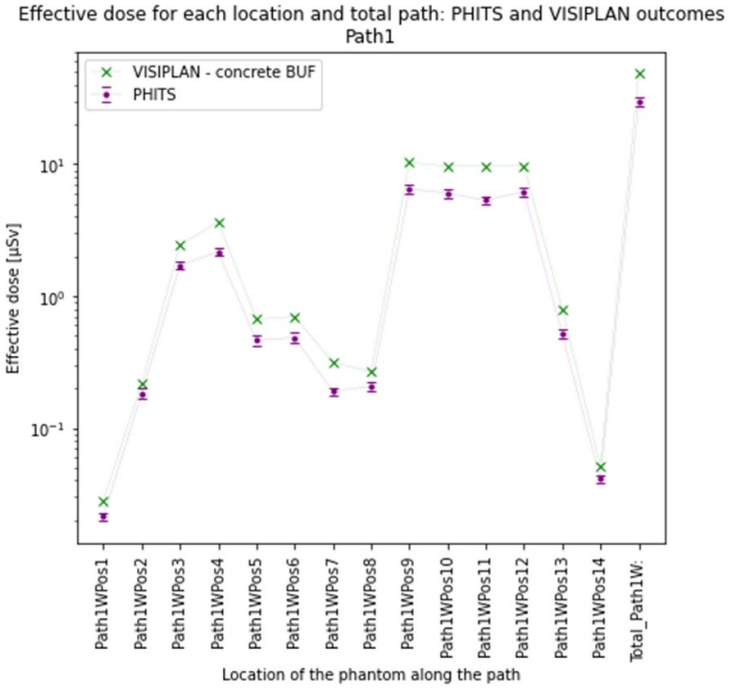


Figure 7. Effective dose for each location and total path: PHITS and VISIPLAN outcomes — Path 1.

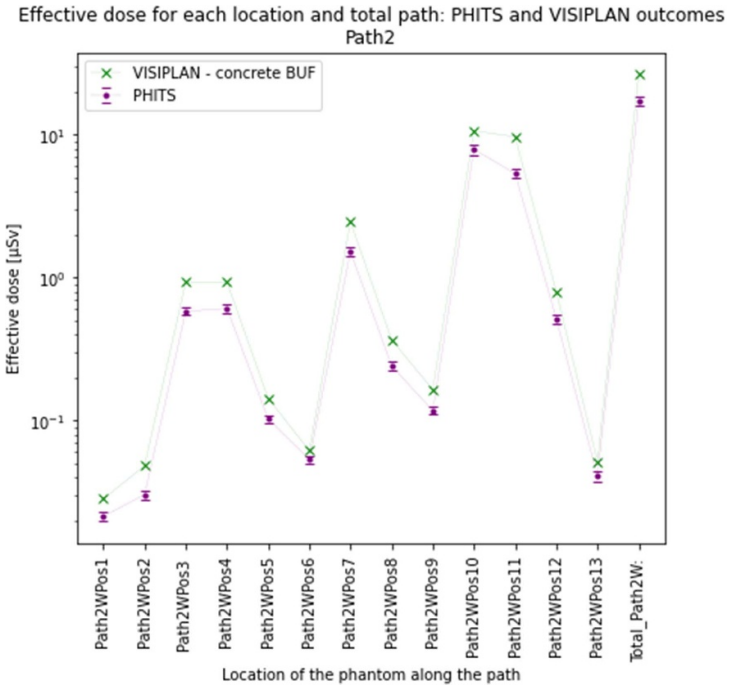


Figure 8. Effective dose for each location and total path: PHITS and VISIPLAN outcomes — Path 2.

Table 2. Comparison of effective dose values for the two analysed paths.

Software	Path 1: total E (μSv)	Path 2: total E (μSv)
PHITS	30	17
VISIPLAN concrete BUF	48	26
Total time in each path (min)	22	20

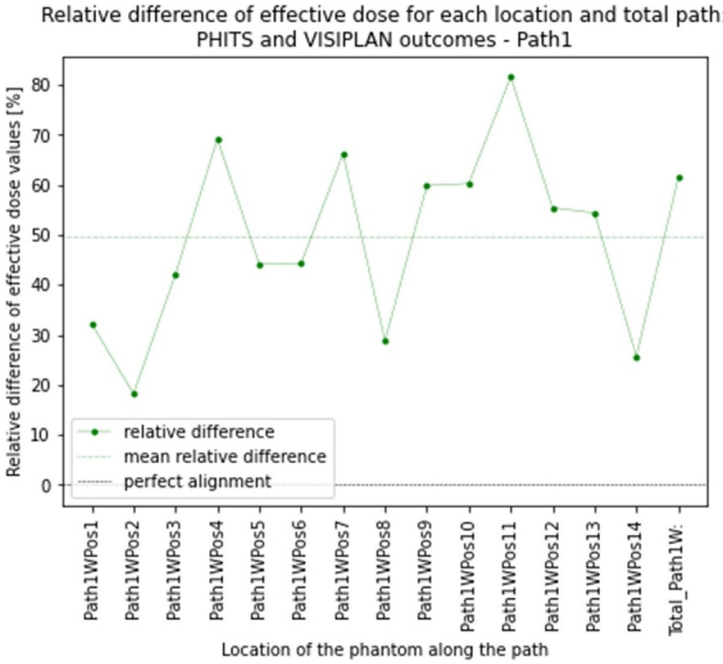


Figure 9. Relative difference of effective dose for each location and total path among PHITS and VISIPLAN results — Path 1.

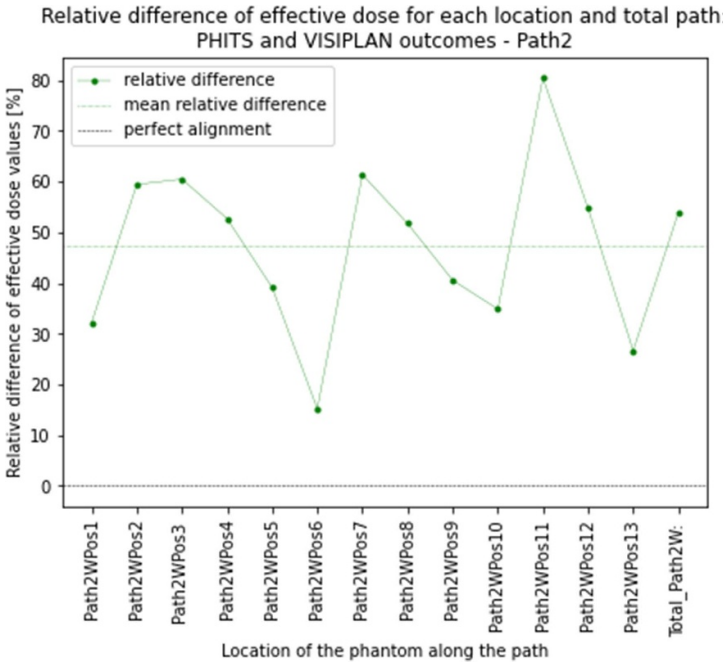


Figure 10. Relative difference of effective dose for each location and total path among PHITS and VISIPLAN results — Path 2.

the storage facility. However, a linear correlation cannot probably be met in the latter configuration, since multiple sources and shielding materials were present at the same time, contributing to a more inhomogeneous radiation field.

Eventually, a comparison of the computation times taken by both methodologies is shown in figure 11. The time for the simulations in VISIPLAN is reported for the cases involving the BUF of concrete, disregarding the time necessary for the simulations with other BUFs. VISIPLAN simulations were run on an average-performance personal laptop on a single core CPU, while PHITS simulations were run on a more powerful personal computer, thus the reported time is the total time to run the simulations on 8 cores in parallel. The total time necessary to calculate the effective dose value for only one

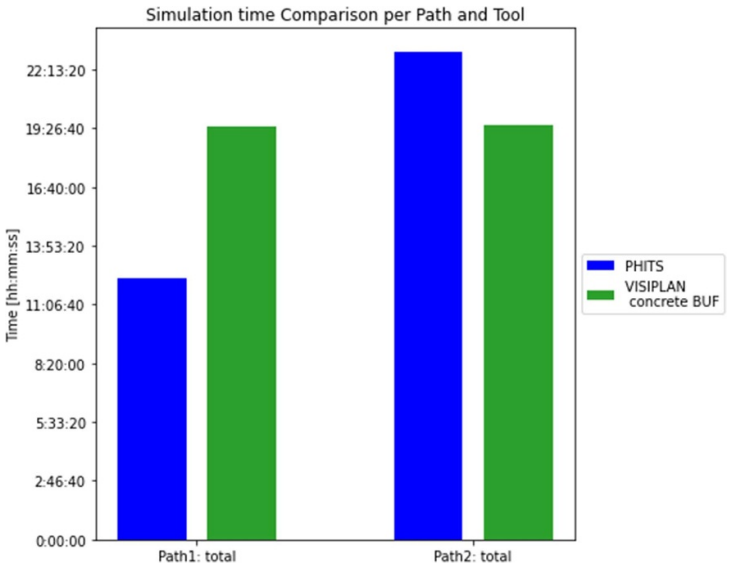


Figure 11. Computational time comparison between PHITS 3.31 and VISIPLAN 4.0 for the total paths simulation.

BUF introduced in VISIPLAN was longer, for Path 1, or shorter, for Path 2, relative to the time spent by the MC calculations. The difference in total simulation time between the first and second path, for PHITS, depended on the number of particles necessary to be simulated to reach the targeted statistical accuracy. In general, the number of necessary particles to simulate increased with the distance between the high-activity barrel and the phantom location, and consequently the corresponding computational time. Nonetheless, a similar consideration can be made for VISIPLAN: including just 1 or 110 points source, the simulation time would have been almost instantaneous, vice versa the integration of 32 000 sampling points for each source led to comparable simulation time with PHITS.

However, also the time necessary to build and parallelise the simulations has to be taken into account. MC simulations can be run in parallel on several cores, but correct handling of the input files requires a certain level of expertise. On the other hand, VISIPLAN has a more user-friendly interface, nevertheless, it requires a training course to avoid calculation mistakes. Moreover, VISIPLAN jobs cannot be executed in batch mode (series) and cannot be multithreaded (parallel): thus, even if the single simulation time is in general lower in the VISIPLAN implementation, the impossibility to run VISIPLAN jobs in parallel or in series leads to a longer execution time if more scenarios are involved. However, it is important to mention that several studies report instead the fast performance of the PK method for dose assessment, especially if running on GPUs, as reported in [20], regarding the voxelisation of 3D models.

4. Conclusion

In this paper, specific PK (VISIPLAN 4.0) and MC (PHITS 3.31) methodologies have been compared for the dose assessment of a worker exposed to a radiation field in several scenarios. A basic configuration was first implemented, considering a volumetric source in a barrel and a phantom located at a certain distance and, therefore, increasing the complexity up to a simulation of a temporary storage facility with several sources. In the last scenario, the worker was performing the task of moving a radioactive barrel from one location in the room to another, following different trajectories.

Increasing the complexity of the scenarios, it was noticed that at a higher number of materials involved a higher discrepancy was found in the results of the two methodologies, due to the impossibility to handle more BUFs simultaneously in VISIPLAN. This led to an overestimation of the VISIPLAN 4.0 results of 50% with respect to the PHITS dose assessment, in the most complex scenario. However, the general results of the two representative methodologies chosen agreed on the optimal path with regard to the comparison of the two trajectories for the foreseen task.

Regarding the computational aspect, the effort was almost comparable between the two methods when the maximum number of sampling source points (32 000) was included in the VISIPLAN configuration. The simulation time could have been considerably shorter if the recommended number of sampling points was included (110), but due to the variability of the results it was not considered in this

implementation. Eventually, also the time necessary to consider more than one BUF and more than one irradiation geometry per scenario increases the time to run multiple simulations.

The PK method is therefore an appropriate choice for obtaining fast results due to its calculation process, if the relevant parameters are correctly chosen. Moreover, the PK method is able to identify the optimal path when different paths are available, in an ALARA assessment, although being conservative. However, in this scenario, the VISIPLAN 4.0 implementation showed intrinsic configuration limitations that lead to slower performance, although this is not representative of the PK method itself. Lastly, the possibility to introduce the ICRP phantom in the MC methodology could be particularly useful in some situations where an inhomogeneous radiation field is present.

In conclusion, for the scenario introduced in this paper, MC appeared to be the more justified choice for the ALARA calculation, with respect to VISIPLAN 4.0, due to the complexity of the configuration (also including the ICRP phantom) and the computational time necessary for the simulations. Nevertheless, for the preliminary assessment of ALARA, PK remains a well-established, fast, and user-friendly methodology.

Data availability statement

All data that support the findings of this study are included within the article (and any supplementary files).

ORCID iDs

Federica Roberto 0009-0001-2457-3300
Mahmoud Abdelrahman 0000-0002-0774-3478
Lombardo Pasquale 0000-0001-7095-7295
Filip Vanhavere 0000-0003-3813-0858
John A Lee 0000-0001-5218-759X

References

[1] International Atomic Energy Agency 2021 *Occupational Radiation Protection During the Decommissioning of Nuclear Installation* (*IAEA TECDOC Series*) (International Atomic Energy Agency) p IAEA-TECDOC-1954
[2] International Atomic Energy Agency 2021 11.3 the ALARA programme: adapted tools *IAEA Presentations* (International Atomic Energy Agency) (available at: www.iaea.org/sites/default/files/22/05/iaea_2021_11.3_alara_adapted_tools_rf.pdf)
[3] Sun P, Zhang H, Xing L, Zhong B, Ying Y and Shen H 2025 NPTS-PK: a new point-kernel code for fast calculation of 3D gamma radiation field *Radiat. Phys. Chem.* **226** 112329
[4] Vermeersch F 2006 VISIPLAN 3D ALARA planning and communication tool *Scientific Report* (SCK-CEN) pp 16–17
[5] Grove Software *MicroShield: Comprehensive Photon/Gamma Ray Shielding and Dose Assessment Program. Radiation Software* (available at: www.radiationsoftware.com/microshield)
[6] Institute for Energy Technology *VRdose: 3D ALARA Planning & Briefing Software* (available at: https://ife.no/en/service/hvrc-vrdose)
[7] Siebert B R L and Thomas R H 1997 Computational dosimetry *Radiat. Prot. Dosim.* **70** 371–8
[8] Kulesza J A 2022 *Mcnp Code Version 6.3.0 Theory & User Manual* (Los Alamos National Laboratory Tech)
[9] Agostinelli S *et al* 2003 Geant4—a simulation toolkit *Nucl. Instrum. Methods Phys. Res. A* **506** 250–303
[10] Sato T *et al* 2024 Recent improvements of the particle and heavy ion transport code system—PHITS version 3.33 *J. Nucl. Sci. Technol.* **61** 127–35
[11] Bednár D, Ličtjak M, Slimák A and Nečas V 2019 Comparison of deterministic and stochastic methods for external gamma dose rate calculation in the decommissioning of nuclear power plants *Ann. Nucl. Energy* **134** 67–76
[12] Listjak M, Ondrej O S, Kubovicocá D, Vermeersch F 2008 Buildup factors for Multilayer shieldings in deterministic methods and their comparison with Monte Carlo *Environment, a.s.* pp 193–6
[13] ICRP 2009 Adult reference computational phantoms. ICRP Publication 110 *Ann. ICRP* **39**(2) 16, 18, 27
[14] ICRP 2010 Conversion coefficients for radiological protection quantities for external radiation exposures. ICRP Publication 116 *Ann. ICRP* **40**(2–5) 35, 36, 47, 48
[15] ICRU 1998 Conversion coefficients for use in radiological protection against external radiation *ICRU Report* 57 (ICRU)
[16] ICRP 2007 The 2007 recommendations of the International Commission on Radiological Protection. ICRP Publication 103 *Ann. ICRP* **37**(2–4)
[17] Vermeersch F 2005 ALARA pre-job studies using the VISIPLAN 3D ALARA planning tool *Radiat. Prot. Dosim.* **115** 294–7
[18] ANSI/ANS-6.4.3 1991 *Gamma Ray Attenuation Coefficient and Buildup Factors for Engineering Materials* (American Nuclear Society)
[19] ICRP 2015 Corrigenda of conversion coefficients for radiological protection quantities for external radiation exposures *Ann. ICRP* **44**(1) 128–35
[20] Xu Z, Li M, Zou B and Yang M 2023 A GPU-based point-kernel gamma dose rate computing code for virtual simulation in radiation-controlled area *Nucl. Eng. Technol.* **55** 1966–73